The Nature of the Ionising Background at $z \approx 2.5 - 5$

Aaron Sokasian[1]

Tom Abel[2] and Lars Hernquist[3]
Department of Astronomy, Harvard University, Cambridge, MA 02138

ABSTRACT

Using radiative transfer calculations and cosmological simulations of structure formation, we study constraints that can be placed on the nature of the cosmic ultraviolet (UV) background in the redshift interval $2.5 \lesssim z \lesssim 5$. Our approach makes use of observational estimates of the opacities of hydrogen and singly ionised helium in the intergalactic medium during this epoch. In particular, we model the reionisation of HeII by sources of hard ultraviolet radiation, i.e. quasars, and infer values for our parameterisation of this population from observational estimates of the opacity of the HeII Lyman-alpha forest. Next, we estimate the photoionisation rate of HI from these sources and find that their contribution to the ionising background is insufficient to account for the measured opacity of the HI Lyman-alpha forest at a redshift $z \sim 3$. This motivates us to include a soft, stellar component to the ionising background to boost the hydrogen photoionisation rate, but which has a negligible impact on the HeII opacity.

In order to simultaneously match observational estimates of the HI and HeII opacities, we find that galaxies and quasars must contribute about equally to the ionising background in HI at $z \simeq 3$. Moreover, our analysis requires the stellar component to rise for $z > 3$ to compensate for the declining contribution from bright quasars at higher redshift. This inference is consistent with some observational and theoretical estimates of the evolution of the cosmic star formation rate. The increasing dominance of the stellar component towards high redshift leads to a progressive softening of the UV background, as suggested by observations of metal line absorption. In the absence of additional sources of ionising radiation, such as mini-quasars or weak active galactic nuclei, our

[1]asokasia@cfa.harvard.edu

[2]hi@tomabel.com

[3]lars@cfa.harvard.edu

results, extrapolated to $z > 5$, suggest that hydrogen reionisation at $z \sim 6$ mostly likely occurred through the action of stellar radiation.

Subject headings: radiative transfer – diffuse radiation – intergalactic medium – galaxies: quasars

1. INTRODUCTION

Determining the relative contributions of different sources to the cosmic ultraviolet background is essential for understanding the evolution of the intergalactic medium (IGM). In particular, this metagalactic radiation field is believed to have reionised hydrogen at $z \sim 6$ (e.g. Becker et al. 2001) and helium slightly later, although the epoch of helium reionisation has yet to be determined observationally (for a discussion, see e.g. Sokasian et al. 2002). Evidence from measured temperature changes, optical depth variations, and evolution in the relative abundances of metal line absorbers strongly suggests that most intergalactic helium became fully ionised at redshifts close to ~ 3.2 (e.g. Davidsen et al. 1996, Jakobsen et al. 1994, Kriss et al. 2001, Reimers et al. 1997, Songaila 1998, Ricotti, Gnedin & Shull 1999, Theuns et al. 2002a, Theuns et al. 2002b, Bernardi et al. 2002 and references therein).

An important probe of the physical state of the intergalactic medium is provided by bright objects at great distances, such as quasars. For example, it is now believed that absorption by diffuse, cosmologically distributed gas is responsible for the hydrogen Lyman alpha forest (e.g. Cen et al. 1994; Zhang et al. 1995; Hernquist et al. 1996). Similarly, Lyα absorption by He II along a line of sight to a distant quasar probes gas in the intervening IGM at even lower overdensities (Croft et al. 1997), characteristic of much of the baryonic matter in the Universe (e.g. Davé et al. 2001; Croft et al. 2001). At a given redshift, the number and strengths of these spectral features is sensitive to the local density of absorbing atoms, which in turn depends on the gas density, cosmological parameters, and the intensity of the ionising background. In fact, much of the interpretation of spectroscopic observations of high redshift quasars relies strongly on this simple picture of the Lyman alpha forest.

Specifically, given a model for the formation of large-scale structure, the number of lines detected in the Lyman-α forest as a function of redshift directly constrains the evolution and spectral properties of the radiation field. In a recent study, Kim, Cristiani, & D'Odorico (2001) showed that the number of lines per unit redshift, dN/dz, with column densities in the interval $N_{\rm H\,I} = 10^{13.64-16}$ decreases continuously from $z \sim 4$ to $z \sim 1.5$ according to $dN/dz \propto (1+z)^{2.19\pm0.27}$. Combined with the results of Weymann et al. (1998), who find

a much flatter distribution for $dN/dz \propto (1+z)^{0.16\pm0.16}$ at $z < 1$, it appears that the line number density of the Lyα forest is well described by a double power-law with a break at $z \sim 1$. These results suggest that the evolution of the forest above $z > 1.5$ is governed mainly by Hubble expansion and that there is little change in the ionising background until the break occurring at $z \sim 1$.

The location of the observed break, however, is inconsistent with theoretical predictions derived from numerical simulations. In particular, studies of the Lyman-α forest carried out by Davé et al. (1999) and Machacek et al. (2000) predict a break in the double power-law occurring near $z \sim 1.8$. While these simulations have provided a successful general description of the evolution of the Lyman-α forest, their apparent inability to match the location of the break indicates that the underlying assumptions regarding the form of the UV background may be incorrect. More specifically, these simulations assume a quasar (QSO) type source population mainly responsible for producing the radiation field. Since the emissivity of quasars is known to fall off steeply below $z \sim 2$, so would their contribution to the UV background, thereby producing a break in dN/dz around this redshift. One way to reconcile the inconsistency between the simulations and observations is to appeal to other types of sources to maintain the intensity of the UV background at a relatively high level until $z \sim 1$.

Recently, Bianchi et al. (2001) have explored the possibility that galaxies might provide this additional contribution to the radiation field. In particular, they derived the H I ionising background resulting from the integrated contribution of quasars and galaxies, taking into account the opacity of the intervening IGM. The quasar emissivity was derived from fits to an empirical luminosity function, while a stellar population synthesis model and a cosmic star-formation history from UV observations were used to estimate the galaxy emissivity. They found that the break at $z \sim 1$ implied by the Kim et al. (2001) analysis can be understood if the contribution from galaxies is comparable to or larger than that of quasars. This is consistent with other determinations of the galactic component of the background (Giallongo, Fontana, & Madau 1997; Devriendt et al. 1998; Shull et al. 1999; Steidel, Pettini, & Adelberger 2001). A significant contribution to the radiation field from galaxies would imply a considerable softening of its spectrum compared to previous models which included only quasars as the dominant source of the ionising metagalactic flux.

In this paper, we shift the focus to higher redshifts to see whether including an additional component from galaxies together with a realistic quasar model is capable of producing the required ionising intensity to match observations of H I photoionisation rates in the redshift range $2.5 < z < 5$. Our method involves combining numerical and empirical results on the reionisation of singly ionised helium (He II) by quasars as a tool

for estimating the additional contribution from galaxies to the background which would be necessary to simultaneously match results derived from the H I Lyα forest. In particular, we select a quasar model based on the study conducted in our earlier paper (Sokasian, Abel & Hernquist 2002; hereafter SAH), where we applied a numerical method to study the 3D reionisation of He II by quasars. The adopted model is then used to calculate the contribution to the H I background from quasars only. We can then estimate the required contribution from galaxies to match the H I photoionisation rates measured by Rauch et al. (1997) in the redshift range $2.5 < z < 5$. Consequently, this approach allows us to make estimates of the amplitude and evolution of this component.

This paper is organised as follows. In Sections 2, 3, and 4 we describe our approach for calculating the emissivities of quasars, galaxies, and recombination radiation from the IGM, respectively. The procedure for determining the ionising background for hydrogen given these emissivities is presented in Section 5. Results of our analysis are discussed in Section 6 and conclusions are given in Section 7.

2. METHOD

In this section we describe our motivation for adopting a specific QSO model for the purpose of deriving the associated contribution to the H I ionising background. This component may be estimated from a QSO luminosity function (LF). However, this requires making a number of assumptions concerning the emission from the sources and how easily this radiation can escape into the IGM. Instead, we will constrain the quasar component of the ionising background by appealing to numerical modeling of He II reionisation along with observational estimates of the evolution of the He II opacity.

To this end, we compile a list of quasar type sources which were selectively extracted from a cosmological simulation according to a QSO LF and a set of characteristic source parameters. This approach provides us with a source list which is directly applicable as input for a cosmological radiative transfer simulation designed to examine the He II reionisation process (as in SAH). The advantage of such an approach is that it provides us with a way of choosing the most successful model for our analysis based on a comparative study between the numerical and empirical results for the He II opacities measured in quasar spectra.

The numerical scheme used to calculate the 3D reionisation of He II by quasars is described in Sokasian, Abel, & Hernquist (2001). In SAH, we used this approach to explore the parameter space associated with the characteristics of the sources and studied how they

influenced global properties of the reionisation process. Comparisons with observational results were made possible by extracting synthetic spectra from the simulations. There our aim was twofold: to develop an understanding of the sensitivity of the reionisation process to source properties and to examine the predictions of the different models in light of recent observational results.

The cosmological simulation we used in SAH was based on a smoothed particle hydrodynamics (SPH) treatment, computed using the parallel TreeSPH code GADGET developed by Springel, Yoshida & White (2001). The particular cosmology we examine is a ΛCDM model with $\Omega_{\rm b} = 0.04$, $\Omega_{\rm DM} = 0.26$, $\Omega_\Lambda = 0.70$, and $h = 0.67$ (see, e.g., Springel, White & Hernquist 2001). The simulation uses 224^3 SPH particles and 224^3 dark matter particles in a 67.0 Mpc/h comoving periodic box, resulting in mass resolutions of $2.970 \times 10^8\ M_\odot/h$ and $1.970 \times 10^9\ M_\odot/h$ in the gas and dark matter components, respectively. The gas can cool radiatively to high overdensity (e.g. Katz, Weinberg & Hernquist 1996) and is photoionised by a diffuse radiation field which is assumed to be of the form advocated by Haardt & Madau (1996; see also, Davé et al. 1999). When sources are included in our treatment of helium reionisation, the ionisation state of the helium is recalculated, ignoring the diffuse background that was included in the hydrodynamical simulation (see Sokasian et al. 2001 for details).

2.1. The QSO model

In SAH, QSO models were differentiated from one another based on their respective values for the free parameters associated with the source selection algorithm. The full details of our scheme are described in §2 and §3 of SAH. The basic procedure involves identifying dense clumps of gas in the cosmological simulations which represent plausible quasar sites, and adopting a prescription for selecting a subset of these objects as actual sources according to an empirical quasar luminosity function. In our analysis, we choose the double power-law form of the quasar luminosity function presented by Boyle et al. (1988) using the open-universe fitting formulae from Pei (1995) for the B-band (4400 Å rest-wavelength) LF of observed quasars, with a rescaling of luminosities and volume elements for our ΛCDM cosmology. Our selection algorithm requires us to adopt an evolving mass-to-light ratio, $\xi(z)$, which scales with z as the break luminosity L_z inherent in the LF.

Once a source with mass, M, has been selected, it is assigned a B-band luminosity, $L_B = M/\xi(z)$ (in ergs s^{-1}). Along with an assumed spectral form, this luminosity is then used to compute the amount of ionising flux that will be generated while the source is active. For all sources, we assume a piece-wise power-law form for the spectral energy

distribution (SED),

$$L(\nu) \propto \begin{cases} \nu^{-0.3} & (2500 \text{ Å} < \lambda < 4400 \text{ Å}); \\ \nu^{-0.8} & (1050 \text{ Å} < \lambda < 2500 \text{ Å}); \\ \nu^{-\alpha_{\rm QSO}} & (\lambda < 1050 \text{ Å}), \end{cases} \quad (1)$$

where a choice of $\alpha_{\rm QSO} = 1.8$ corresponds to the SED proposed by Madau, Haardt, & Rees (1999) based on the rest-frame optical and UV spectra of Francis et al. (1991) and Sargent, Steidel, & Boksenberg (1989), and the EUV spectra of radio-quiet quasars (Zheng et al. 1998).

The entire selection process, including the assigning of intensities, introduces five free parameters associated with source characteristics. They are: (1) a universal source lifetime, $T_{\rm life}$, (2) a minimum mass, $M_{\rm min}$, (3) a minimum luminosity at $z = 0$, $L_{\rm min,0}$, (4) an angle specifying the beaming of the bi-polar radiation, β, and (5) a tail-end spectral index, $\alpha_{\rm QSO}$, in the regime $\lambda < 1050$ Å. In SAH, we computed and analysed six models with different sets of values for the free parameters. Below, we discuss the parameter choices for Models 1 and 5 which represent our fiducial and *best fit* models, respectively. Table 1 lists the corresponding parameter choices.

In Model 1, our fiducial case, we adopted a widely quoted value for $L_{\rm min,0}$ based on the results of Cheng et al. (1985) who show that the LF of Seyfert galaxies (which is well correlated with that of optically selected quasars at $M_B = -23$) exhibits some evidence of leveling off by $M_B \simeq -18.5$ or $L_{\rm min} \simeq 3.91 \times 10^9\ L_{B,\odot}$ at $z = 0$. The tail-end spectral index parameter for this model was chosen to be $\alpha = 1.8$, making the SED in this model identical to the one advocated by Madau, Haardt, & Rees (1999). In Model 5, we examined the effect of reducing the ionising emissivity from the sources. This was accomplished by increasing $L_{\rm min,0}$ by a factor of six and by steepening the tail-end spectral index to $\alpha = 1.9$. In both models, the sources are assumed to radiate their flux isotropically ($\beta = \pi$) and to have a minimum mass cut off of $M_{\rm min} = 1.80 \times 10^{10}\ M_\odot$, which produces good agreement with the B-band emissivity predicted by the LF and which provides a realistic mass function given the level of resolution of the simulation at this mass limit (see SAH for further details). The value of the mass cut off is also consistent with the assumption that the sources are galaxy type objects acting as quasar hosts.

Figure 1 shows the redshift evolution of the effective mean optical depth for He II absorption derived from both models. The mean optical depth is defined as $\bar{\tau}_{\rm He\ II} \equiv -\log_e \langle T \rangle$, where T is the transmittance extracted from the synthetic spectra from each model. The average is performed over 500 lines of sight within 35 wavelength bins of width $\Delta\lambda = 6.57$ Å. Hatched regions represent the optical depth derived from the

simulations at the 90% confidence level with the dashed lines indicating mean values. For comparison, we also plot the opacities measured at different redshifts in the spectra of Q 0302-003 (Heap et al. 2000), PKS 1935-692 (Anderson et al. 1999, reported values come from Smette et al. 2002 who perform an optimal reduction of the whole data set), and HE 2347-4342 (Smette et al. 2002). It is clear from this figure that Model 5 provides a much better match to the observational results. This model also predicts full He II reionisation by $z \simeq 3.4$, a result consistent with the recent analysis conducted by Theuns et al. (2002) who show clear evidence for a sudden decrease in the effective optical depth in H I at the same redshift due to the temperature increase associated with He II reionisation. In the analysis presented in this paper, we will adopt Model 5 as our most promising quasar model, based on its predictions for the evolution of the He II opacity. In §7, however, we summarise the related degeneracy associated with successful quasar models and discuss the resulting implications in the context of our study.

Given our QSO model, the *emergent* emissivity at each redshift is calculated by summing up the B-band emissivity (in ergs s^{-1} Hz^{-1} cm^{-3}) contributions from each source and then using the universal SED to derive the following expression for $\lambda < 1050$ Å:

$$\epsilon_{\rm QSO}(\nu, z) \simeq 0.423\ \epsilon_{\rm QSO}(\nu_B, z)\left(\frac{\nu}{\nu_{1050}}\right)^{-1.9}, \qquad (2)$$

where the numerical pre-factor accounts for the spectral mapping from the blue frequency, ν_B, to the frequency evaluated at $\lambda = 1050$ Å, ν_{1050}. In the following section, we describe our prescription for adding a component from galaxies and define an expression for its emissivity.

3. GALAXIES

Galaxies will represent the second class of sources which we allow to contribute to the H I ionising background. We assign a spectral profile of the form $f(\nu) \propto \nu^{-\alpha_{\rm GAL}}$ for $\lambda < 912$Å to these sources. In this paper we assume $\alpha_{\rm GAL} = 5$, which is widely regarded as a realistic value based on spectral studies of stellar atmospheres. The much steeper spectral slope relative to quasars means that galaxies produce an insignificant number of He II ionising photons for any reasonable luminosity model. This result justifies our approach of relying on an He II reionisation simulation which contains only quasars. We emphasise that our conclusions are insensitive to the value adopted for $\alpha_{\rm GAL}$ as long as galaxies contribute negligibly to He II reionisation.

The next step is to adopt a functional form describing the redshift evolution of the

emissivity of this component. Here we make the assumption that the emissivity responsible for the ionising UV background from this component is directly proportional to the inherent star formation rate (SFR) within the galaxies. This is a fair premise since the SFR is a direct tracer of the young OB stars which are the dominant producers of H I ionising photons in galaxies. This assumption allows us to utilise empirical measurements of the SFR at various redshifts as a basis for modeling the redshift evolution of the emissivity within the redshift range in question. In the future, it will also be interesting to contrast this with an analysis of direct theoretical predictions of the SFR (e.g. Nagamine et al. 2000, Springel & Hernquist 2002a). For our present purposes it is convenient to parameterise the comoving *emergent* emissivity from galaxies using the following expression:

$$\epsilon_{\rm GAL,c}(\nu, z) = \epsilon_{\rm GAL,c}(\nu_{\rm HI}, 3)\ f(z)\ \left(\frac{\nu}{\nu_{\rm HI}}\right)^{-\alpha_{\rm GAL}}, \tag{3}$$

where $\epsilon_{\rm GAL,c}(\nu_{\rm HI}, 3)$ represents the comoving emissivity from galaxies at the hydrogen ionisation frequency $\nu_{\rm HI}$ at $z = 3$ and $f(z)$ is a dimensionless redshift dependent function which is normalised to unity at $z = 3$. The function $f(z)$ can then serve to characterise the evolution of a particular galactic model while the value of $\epsilon_{\rm GAL,c}(\nu_{\rm HI}, 3)$ provides an overall normalisation.

In Figure 2, we present extinction-corrected data points for the comoving SFR in a flat Λ cosmology with parameters $(\Omega_m, \Omega_\Lambda)$=(0.37, 0.63) and $h = 0.7$, as provided by Nagamine, Cen, & Ostriker (2000). While not identical to the cosmology we employ, that of Nagamine et al. is very similar to ours and their summary of the observations is thus adequate for our present purposes. As is apparent, the sparse and loosely constrained observations beyond a redshift $z \sim 2$ hardly warrant any attempt to fit the data as a means to derive $f(z)$. Rather, we chose the simple form $f(z) = 10^{m(z-3)}$ and consider two values for the slope, m, which represent the subject of recent debates as to whether the SFR continues to slightly rise or fall off beyond $z \sim 3$ (see, e.g. Madau et al. 1996, Steidel et al. 1999). These models are indicated by the bold short-dashed and long-dashed lines in Figure 2, which we refer to as our galactic Model 1 (M1: m=-0.260) and galactic Model 2 (M2: m=0.135) respectively. Our choices for the slopes in these two cases are somewhat arbitrary, but they roughly bracket the observations and will, therefore, enable us to gauge the impact of a rising or falling SFR at $z > 3$ in the context of the analysis conducted in this paper. In both of these models, we set $\epsilon_{\rm GAL,c}(\nu_{\rm HI}, 3) = 3.6 \times 10^{-49}$ ergs s^{-1} Hz^{-1} cm^{-3} which is roughly 9% smaller than the corresponding quasar contribution. We discuss the motivation behind this choice in §6 where we present results for the photoionisation rates.

4. RECOMBINATION RADIATION FROM THE IGM

Recombination radiation from the ionised IGM can also provide a significant contribution to the ionising background. In particular, Haardt & Madau (1996) have shown that this component can provide a fair fraction of the ionising photons at redshifts near $z \sim 3$. For helium, only recombinations to the ground level of He II are able to contribute to the diffuse He II ionising background. The helium reionisation simulation used in this paper includes an approximate treatment to account for this component which is directly incorporated into the radiative transfer calculations (see §3.1.3 of Sokasian et al. 2001).

For hydrogen, the following processes contribute to the diffuse ionising background: (1) recombinations to the ground state of H I, (2) He II Lyα emission ($2^2P \longrightarrow 1^2S$) at 40.8 eV, (3) He II two-photon ($2^2S \longrightarrow 1^2S$) continuum emission, (4) and He II Balmer continuum emission at $\geq$ 13.6 eV. We ignore the contribution of He I and He II recombination to the hydrogen ionising background. In the case of the former, this is motivated by the relative smallness of the $n_{\rm HeI}/n_{\rm HeII}$ and $n_{\rm HeI}/n_{\rm HI}$ ratios encountered in typical intergalactic gas which has been photoionised by galaxies and quasars. For the latter, the exclusion is motivated by the fact that the relative cross section for absorption of photons with energies $\geq$54.4 eV is much larger for He II than H I. Coupled with the fact that the typical ratio for $n_{\rm HeIII}/n_{\rm HI}$ encountered in the photoionised IGM is large, we find that within the context of our analysis it is safe to make the approximation that all the photons released from recombinations to the ground state of He II are absorbed by nearby He II ions before they have a chance to ionise H I atoms.

For the purposes of this paper, we find that it is sufficient to use global number densities representative of the IGM to approximate the corresponding emissivity from the relevant processes. In order to properly account for the inhomogeneity of the IGM, we compute global volume-averaged clumping factors from radiative transfer grid at each redshift, $C_f(z)$, which we then incorporate into the relevant expressions. We discuss the details associated with these calculations in the following sections.

4.1. Radiative Recombinations

Given the electron number density, n_e, and the ion number density n_i, the emissivity from direct recombinations to the n^2L level for hydrogen-like atoms with atomic number Z and ionisation threshold frequency ν_{th} from a photoionised gas that is in local thermodynamic equilibrium at temperature, T, can be computed using the Milne relation

(Osterbrock 1989) which yields

$$\epsilon_{fb}(\nu) = \frac{4\pi}{c^2}\left(\frac{h^2}{2\pi m_e kT}\right)^{3/2} n_e n_i \frac{2n^3}{Z^3} h\nu^3 \sigma_{\rm HI}(\nu/\nu_{th}) e^{-h(\nu-\nu_{th})/kT}, \quad (4)$$

where $\sigma_{\rm HI}(\nu/\nu_{th})$ is the frequency dependent hydrogen photoionisation cross section, h and k are the Plank and Boltzmann constants, respectively, m_e is the electron mass, and c is the speed of light. Following the reasoning in Sokasian et al. (2001) we artificially set all temperatures for the ionised gas to $T = 2.0 \times 10^4 K$ as a correction to the SPH temperatures which exclude the extra heating introduced by radiative transfer effects (see Abel & Haehnelt 1999). As a further approximation, we set $\sigma_{\rm HI}(\nu/\nu_{th}) = \sigma_{{\rm HI},o}(\nu/\nu_{th})^{-3}$ where $\sigma_{{\rm HI},o} = 6.30 \times 10^{-18}$ cm^2 is the photoionisation cross section at the Lyman limit for H I (Osterbrock 1989).

To compute realistic values for the recombination emissivity, we require information regarding the clumping statistics associated with the IGM. In the context of our calculation, this will reduce to a global volume-averaged clumping factor for each redshift, $C_f(z)$, which we can then use as a multiplicative prefactor in the above expression. In order to obtain reliable values for the clumping factor of the IGM from our radiative transfer grid, it is necessary to discount cells harbouring collapsed objects with cold gas that are not part of the IGM but which can significantly alter the clumping statistics. We achieve this by considering only cells below a specific overdensity cut-off. The choice for the cut-off is somewhat arbitrary since the distinction between the IGM and collapsed objects is blurred. In this paper, we employ scatter plots showing the density vs. temperature for the SPH particles (see, e.g., Davé et al. 1999 or Springel & Hernquist 2002b) to estimate this cut-off. In particular, these plots show a bifurcation between the reservoir of underdense cool gas (i.e. the IGM) and shock-heated gas of moderate density or cold high density gas in collapsed objects which occurs somewhere between an overdensity of $10 - 50$, independent of redshift. In our analysis, we adopt a median value of 30 for our overdensity cut-off at all redshifts. This value results in an exclusion of only 0.14% of the volume and a global volume averaged clumping factor of 3.88 at $z = 3$. Adopting an overdensity cut-off of 10 (50) would lead to a -32% ($+27\%$) change in the clumping factor at the same redshift. Although only 0.14% of the volume is excluded at $z = 3$ with the adopted value for the cut-off, the corresponding mass harboured in these excluded cells corresponds to roughly 11.5% of the total mass in the simulation volume. For consistency, we exclude the corresponding *collapsed-mass* at each redshift when deriving n_e and n_i.

We note that our estimates for the clumping factor are considerably smaller than those of Springel & Hernquist (2002a; as summarised by e.g. their Figure 16), because here we exclude high density regions from our estimate of $C_f(z)$. This is appropriate because in this

paper we are interested in the volume averaged properties of the IGM at a redshift when the Universe was essentially optically thin to hydrogen ionising photons, while Springel & Hernquist (2002a) were concerned with the situation leading to hydrogen reionisation when most of these photons would have been absorbed in the vicinity of the sources which produced them. In any event, as indicated above, a modest increase in the overdensity threshold would have a similarly modest impact on the clumping factor and the inferred emissivity from radiative recombination.

For simplicity, the latter densities are approximated by assuming complete ionisation ($n_i/n_{\rm tot} = 1$) within the photoionised regions. This approximation is certainly justified in comparison to other uncertainties present in our analysis. The relevant densities are thus given by,

$$n_e(z) = 2n_{He,{\rm tot}} I_{\rm HeIII} + n_{H,{\rm tot}} I_{\rm HII}(z) \tag{5}$$

$$n_{\rm HI}(z) = n_{H,{\rm tot}} I_{\rm HII}(z) \tag{6}$$

$$n_{\rm HeIII}(z) = n_{He,{\rm tot}} I_{\rm HeIII}(z) \tag{7}$$

where $n_{i,{\rm tot}}$ represents the total number density of species i averaged over the entire simulation box (excluding the collapsed-mass as defined above), and $I_i(z)$ is the fraction of the volume which has become ionised in species i by redshift z. In the case of He III, $I_{\rm HeIII}(z)$ is extracted directly from the helium simulation results. For H II, we approximate $I_{\rm HII}(z)$ as the ratio of the cumulative number of H I ionising photons that were released by quasars and galaxies by redshift z to the total number of hydrogen atoms present in the IGM (which again excludes the collapsed-mass fraction). Obviously, we restrict the maximum value of $I_{\rm HII}(z)$ to unity. It is also important to point out that we limit contributions to the H I ionising pool only to photons with frequencies in the range $\nu_{\rm HI} < \nu < \nu_{\rm HeII}$ under the earlier premise that photons with frequencies $\nu > \nu_{\rm HeII}$ are immediately absorbed in the IGM by the He II ions.

4.2. Lyα Emission

Recombinations into He II which end up populating the 2^2P level are converted to Lyα 304 Å photons which are capable of ionising H I. These photons resonantly scatter, and therefore diffuse only slowly away from their point of origin before they are absorbed. As a result, the immediate fate of a He II Lyα photon mainly depends upon the competition between H I continuum absorption and the local opacity at the He II Lyα frequency ν_α (the effect of dust on destroying Lyα radiation is negligible [Haardt & Madau 1996]). For the purposes of our analysis, it is sufficient to assume that all Lyα photons eventually

contribute to the H I ionising background either by scattering enough times to encounter an H I atom in the cloud of origin or eventually redshifting below the line frequency and escaping into the IGM. Which process comes first depends on the velocity gradient versus the absorption coefficient of H I at the He II Lyα frequency. In either case, assuming all the energy is released exactly at the line frequency, the emissivity associated with Lyα line radiation can be written as,

$$\epsilon_{\mathrm{Ly}\alpha}(\nu) = h\nu\delta(\nu - \nu_\alpha) n_{2^2P} A_{2^2P,1^2S}, \tag{8}$$

where $A_{2^2P,1^2S}$ is the transition probability for $2^2P \longrightarrow 1^2S$ transitions in He II and n_{2^2P} is number density of He II ions in the 2^2P state. In our case, the transition probability cancels out in the above expression since we derive n_{2^2P} by assuming the equilibrium condition,

$$0.75\alpha_B n_e n_{\mathrm{HeIII}} = n_{2^2P} A_{2^2P,1^2S}, \tag{9}$$

where the use of the Case B recombination coefficient, α_B, implicitly assumes that all $n > 2$ recombinations will eventually cascade down and populate the $n = 2$ level. For this paper, we use the fitting formula provided by Hui & Gnedin (1997) and arrive at $\alpha_B = 9.089 \times 10^{-13}$ cm^3 s^{-1} for $T = 2.0 \times 10^4 K$. The factor 0.75 represents the fraction of recombinations to the excited states that will eventually populate the 2^2P state based on the degeneracy of available states in the P level (the remainder end up in the 2^2S state). This assumes that the rate of transitions between the S and P states is small, which is valid at the typical densities associated with the IGM.

4.3. Two-Photon Continuum

The radiative decay $2^2S \longrightarrow 1^2S$ in He II is almost entirely due to two-photon emission and is also capable of contributing to the diffuse H I ionising background. The emissivity for this process can be expressed as,

$$\epsilon_{2ph}(\nu) = \frac{h\nu}{\nu_\alpha} A_{2^2S,1^2S}(\nu/\nu_\alpha) n_{2^2S}, \tag{10}$$

where $A_{2^2S,1^2S}(\nu/\nu_\alpha)$ is the frequency dependent transition probability, which again cancels out via the assumption of the equilibrium condition,

$$0.25\alpha_B n_e n_{\mathrm{HeII}} h = n_{2^2S} A_{2^2S,1^2S}, \tag{11}$$

adopted under the premise mentioned in the preceding section.

5. COMPUTING THE IONISING BACKGROUND

Given the emissivities of each component, we can proceed to the calculation of the resulting ionising background intensity and the corresponding photoionisation rate. The cosmological radiative transfer equation for diffuse radiation can be expressed as (see, e.g., Peebles 1993),

$$\left(\frac{\partial}{\partial t} - \nu\frac{\dot{a}}{a}\frac{\partial}{\partial \nu}\right)J = -3\frac{\dot{a}}{a}J - c\kappa J + \frac{c}{4\pi}\epsilon, \tag{12}$$

where a is the scale factor, κ is the continuum absorption coefficient per unit length along the line of sight, and ϵ is the proper space-averaged volume emissivity which in our case can be expressed as the sum $\epsilon(\nu, z) = \epsilon_{\rm QSO}(\nu, z) + \epsilon_{\rm GAL}(\nu, z) + \epsilon_{\rm IGM}(\nu, z)$ where $\epsilon_{\rm IGM}(\nu, z) = \epsilon_{fb}(\nu, z) + \epsilon_{{\rm Ly}\alpha}(\nu, z) + \epsilon_{2ph}(\nu, z)$. The mean specific intensity of the background, J, at the observed frequency ν_o, as seen by an observer at redshift z_o is then,

$$J(\nu_o, z_o) = \frac{1}{4\pi}\int_{z_o}^{\infty}\frac{dl}{dz}\frac{(1+z_o)^3}{(1+z)^3}\epsilon(\nu, z)e^{-\tau_{\rm eff}}\ dz, \tag{13}$$

where $\nu = \nu_o(1+z)/(1+z_o)$ and dl/dz is the proper line element in our ΛCDM cosmology,

$$\frac{dl}{dz} = \frac{c}{H_o(1+z)}[0.3(1+z)^3 + 0.7]^{-1/2}, \tag{14}$$

where c is the speed of light and H_o is the present day Hubble parameter. The remaining exponential term accounts for absorption occurring through dz due to discrete absorption systems which is parameterised by a mean optical depth $\tau_{\rm eff}$ which, for a Poisson-distribution of clouds, can be expressed as:

$$\tau_{\rm eff}(\nu_o, z_o, z) = \int_{z_o}^{z} dz' \int_0^{\infty}\frac{\partial^2 N_{\rm col}}{\partial N_{\rm col,HI}\partial z'}(1 - e^{-\tau})\ dN_{\rm col,HI} \tag{15}$$

(Paresce, McKee, & Bowyer 1980), where $\partial^2 N_{\rm col}/\partial N_{\rm col,HI}\partial z'$ is the redshift and column density ($N_{\rm col}$) distribution of absorbers along a line of sight, and τ is the Lyman continuum optical depth through an individual cloud. The usual form for the redshift and column density distribution of absorber lines is given as:

$$\frac{\partial^2 N_{\rm col}}{\partial N_{\rm col,HI}\partial z} = A_o\ N_{\rm col,HI}^{-1.5}(1+z)^{\gamma}. \tag{16}$$

with A_o and γ acting as fitting parameters. For our analysis here, we choose to fit the above function exactly as in Madau, Haardt, & Rees (1999) where a single redshift exponent, $\gamma = 2$, is assumed for the entire range in column densities with a normalisation value of

$A_o = 4.0 \times 10^7$. At $z = 3$, the adopted values produce roughly the same number of Lyman limit systems and lines above $N_{\rm col,HI} = 10^{13.77}$ cm^{-2} as observed by Stengler-Larrea et al. (1995) and estimated by Kim et al. (1997), respectively. With a single power law describing the distribution of absorbers along a line of sight, the effective optical depth can now be expressed as an analytic function of redshift and frequency (i.e. equation [6] in Madau et al. 1999),

$$\tau_{\rm eff}(\nu_o, z_o, z) = \frac{4}{3}\sqrt{\pi\sigma_{\rm HI,o}}N_o(\nu_o/\nu_{\rm HI})^{-1.5}(1+z_o)^{1.5}[(1+z)^{1.5} - (1+z_o)^{1.5}]. \qquad (17)$$

It is important to note that the expression above for the mean opacity does not explicitly include the contribution of helium to the attenuation. While the opacity due to He I ionisations at 504 Å is negligible in the case of a background composed in part by hard sources like quasars (Haardt & Madau 1996), He II absorption may still contribute a measurable level of opacity for the population of photons with frequencies $\nu > \nu_{\rm HeII}$ (produced almost exclusively by quasars). However, as we shall show below, any additional attenuation due to helium absorption has a very small effect on the H I photoionisation rate and does not affect the results of this analysis; we therefore omit this component.

Given the background intensity $J(\nu, z)$, the global photoionisation rate can then be calculated according to:

$$\Gamma_{\rm HI}(z_s) = \int_{\nu_{\rm HI}}^{\infty} \frac{4\pi J(\nu, z)}{h\nu}\sigma_{\rm HI,o}(\nu/\nu_{\rm HI})^{-3}\, d\nu \qquad (18)$$

where we have a adopted a frequency dependence of $(\nu/\nu_{\rm HI})^{-3}$ for the photoionisation cross section. Here we note that for the quasar model employed in this paper, an integration up to only $\nu_{\rm HeII}$ would have decreased the photoionisation rate by roughly 0.2% at z=3.0. This thus represents the maximum decrement any additional attenuation from helium absorption may cause and is small enough for us to continue with its omission.

6. RESULTS AND DISCUSSION

In Figure 3, we plot the resulting background intensities at $\lambda = 912$ Å for three cases: 1) quasars alone, 2) quasars combined with an M1 galactic component, and 3) quasars combined with an M2 galactic component. In both galactic models, we set $\epsilon_{\rm GAL,c}(\nu_{\rm HI}, 3) = 3.4 \times 10^{-49}$ ergs s^{-1} Hz^{-1} cm^{-3}, which is roughly equal to the corresponding contribution from the quasars at the same redshift. The associated recombination component from the ionised IGM is also included in all three cases. The values plotted for the quasar contribution reflect an average over 20 unique realisations associated with

the quasar section algorithm. The shaded region refers to the Lyman limit background estimated from the proximity effect (Giallongo et al. 1996; Cooke et al. 1997; Scott et al. 2000). Here we see that all three cases produce total intensities that appear to be consistent with measurements, although it is obvious that observational uncertainties are quite large. Nevertheless, it is arguable that the larger intensities associated with the inclusion of the galactic component M2 appear to offer the best agreement with the measurements at $z \gtrsim 3.8$.

The resulting H I photoionisation rate for each of the three cases is plotted in Figure 4. Hatched regions represent the range of values corresponding to the 90% confidence level from the 20 realisations of the quasar sources. The two data points are measurements of $\Gamma_{\rm HI}$ over the indicated redshift ranges (horizontal lines) given by Rauch et al. (1997), who measured the H I Lyα forest absorption from intervening gas in seven high resolution QSO spectra obtained with the Keck telescope. The values of these data points have been adjusted to the cosmology used in this paper. Here we can clearly see that quasars alone, although successful in matching $z \simeq 3$ measurements, fail to produce the observed rates in the range $3.5 < z < 4.5$ by a large factor. The inclusion of the M1 galactic component whose contribution tapers off with redshift, does not appear to do any better and is, in fact, incompatible with the $2.5 < z < 3.5$ measurement as well. Only by including an M2 galactic component do we obtain a reasonable match to the observations.

These conclusions have potential implications for our understanding of recent observations indicating that hydrogen in the Universe was reionised by redshift $z \sim 6$ (e.g. Becker et al. 2001). In particular, from Figure 3c, we see that the background intensity at the hydrogen Lyman limit predicted by our model becomes increasingly dominated by stars for $z > 4$. This suggests that unless there are other sources of ionising radiation present in the real Universe that have been neglected in our analysis, such as mini-quasars or weak active galactic nuclei, hydrogen reionisation at $z \sim 6$ must have been driven mainly by stellar radiation.

The fact that our choice for $\epsilon_{\rm GAL,c}(\nu_{\rm HI}, 3)$ results in a reasonable match to the photoionisation measurements in the latter case is not coincidental as it was specifically chosen for this purpose. To investigate whether this value is reasonable in the context of corresponding measurements of the emissivity of galaxies at larger wavelengths ($\lambda \simeq 1500$ Å) we will need to first adopt a realistic ratio between the flux densities at 1500 Å and 900 Å, $f[1500]/f[900]$. After analysing a composite spectrum of 29 LBGs at $z \sim 3.4$, Steidel et al. (2001) derived an observed ratio of $f[1500]/f[900] \simeq 17.7$. However, it should be emphasised that the LBGs comprising their composite spectrum were drawn from the bluest quartile of intrinsic far-UV colours and may be exhibiting larger than average 900 Å

continuum emission. In fact, more recently, Giallongo et al. (2002) examined the spectra of two galaxies at $z = 2.96$ and $z = 3.32$ which exhibited little or no flux at $\lambda = 900$ Å and were not included in the latter subsample. They derived a lower limit of $f[1500]/f[900] > 71$ which is roughly 4 times the value derived by Steidel et al. (2001).

In Figure 5 we plot the resulting comoving emissivity at $\lambda = 1500$ Å from our galactic model M2 as a function of redshift based on the two values of the observed flux ratio from Steidel et al. (2001) and Giallongo et al. (2002). Also plotted are the relevant observations of the UV emissivity at $\lambda = 1500$ Å from Steidel et al. (1999), Pascarelle et al. (1998), Madau et al. (1996), and Madau et al. (1998) adjusted for a flat ΛCDM cosmology similar to ours. With the exception of the Madau et al. data point at $z = 4$, it appears as if the adopted galactic model M2 offers good agreement with the observations if the typical value for $f[1500]/f[900]$ lies somewhere between the values advocated by Steidel et al. (2001) and Giallongo et al. (2002). This behaviour is consistent with the recent theoretical predictions of Springel & Hernquist (2002a), who find that the SFR in high resolution simulations which include hydrodynamics and a multi-phase model for star forming gas (Springel & Hernquist 2002c) rises from $z = 0$ out to $z \approx 5.4$ before declining at even higher redshifts.

Our value of $\epsilon_{\rm GAL,c}(\nu_{\rm HI}, 3)$ also appears to be consistent with the recent suggestion that LBGs emit a comparable number of ionising photons to QSOs at $z \sim 3$ (Steidel et al. 2001), although we remind the reader that the adopted QSO model (Model 5 from SAH) in this paper has less emission than the "standard" QSO model (Model 1 from SAH), as is required in order to match the He II opacity measurements (see Table 1, Figure 1). More specifically, in the case which combines the adopted QSO model and galactic Model M2 we find $J_{\rm GAL}(\nu_{\rm HI})/J_{\rm QSO}(\nu_{\rm HI}) \simeq 0.77$ at $z \simeq 3$ whereas the same galactic component combined with the standard QSO model would produce $J_{\rm GAL}(\nu_{\rm HI})/J_{\rm QSO}(\nu_{\rm HI}) \simeq 0.47$ at the same redshift. It is interesting to point out that the standard QSO model not only proves to be unsuccessful in matching the helium opacity measurements but would also correspond to an unsuccessful model in the context of the hydrogen photoionisation rate measurements by Rauch et al. (1997). In particular, without any additional contribution from a galactic component, the resulting photoionisation rate from the standard QSO model would overpredict the $2.5 < z < 3.5$ measurement by $\simeq 43\%$ while underpredicting the $3.5 < z < 4.5$ measurement by $\simeq 59\%$. Furthermore, any attempt to include a reasonable contribution from a galactic component, such as in Model M2, would inevitably exacerbate the disagreement at $z \simeq 3$. It therefore appears as if the standard QSO model as defined by the parameters in Table 1 for Model 1 in conjunction with the Pei (1995) B-band fit to the luminosity function presented by Boyle et al. (1988) overpredicts the ionising emissivity in both hydrogen and helium at $z \simeq 3$. This conclusion is consistent with the preliminary analysis of the density of faint QSOs carried out by Steidel et al. (1999) in which their LBG

survey indicated that the standard extrapolated QSO luminosity function may slightly overpredict the QSO contribution to $J(\nu_{\rm HI})$ at $z \sim 3$.

If we are to accept the form and fit to the QSO luminosity function, then the incompatibility between the standard QSO model and observations suggests that either the extrapolation to the faint end or the adopted SED or a combination of both is misrepresented. The extrapolation to faint galaxies is parameterised by the minimum luminosity allowed for the quasars, L_{min}. The widely adopted procedure for estimating L_{min} is based on the idea that present day Seyfert galaxies are counterparts to high redshift quasars and that the faintest luminosities associated with Type I Seyferts should be representative of the minimum luminosities of quasars once a luminosity evolution model has been factored in. A logical choice for the evolution model, which we subsequently adopted in this paper, is based on the observed evolution of the break luminosity in the LF of quasars. However, as the failure of the standard model suggests, adopting the faintest values for $L_{min,0}$ from Seyfert galaxies appears to produce too many faint QSOs and is partly responsible for the apparent overproduction of ionising photons in both H I and He II. The implication then could be that the minimum luminosity evolves separately from the apparent evolution in the break luminosity. A possible motivation for such a scenario could be provided by theories of hierarchical structure formation which are more efficient in inhibiting the formation of the smallest supermassive black holes and/or the accretion rate onto them. Delving into the theory related to such speculations is beyond the scope of this paper; instead we refer the reader the work of Haiman & Menou (2000) and Kauffmann & Haehnelt (2000) which provide a good review of the subject.

With respect to the form for the SED, it is important to point out that the EUV spectral indices observed in quasar spectra exhibit a significant amount of scatter (see, e.g, Zheng et al. 1998, Telfer et al. 2002), which makes it difficult to define a universal index representative of all quasars. This dispersion is apparent in Figure 6 where we show the combined distribution of EUV indices for radio-quiet and radio-loud QSOs from Telfer et al. (2002) (data kindly provided by G. Kriss). The indices in this distribution are defined by $f(\nu) \propto \nu^{-\alpha}$ between 500 and 1200 Å, which is comparable to our definition for α_{QSO}. It is clear from this plot and the corresponding statistics that it is difficult to represent this quantity by a single value appropriate for all quasars. Within this context, our choice of $\alpha_{QSO} = 1.9$ seems entirely plausible. We must note, however, that the situation would be much more convoluted if there existed some correlation between the spectral index and the intrinsic luminosity of the source, as suggested by the strong luminosity evolution in the X-ray and optical wave bands of quasars (see, e.g., Boyle 1994). Recent investigations into this matter (Yuan et al 1998; Brinkmann et al. 1997) have revealed that the observed α-luminosity correlation can be attributed to the dispersion in the observational data points

and is thus not an underlying physical property of the sources.

6.1. Other QSO Models

We have shown that a QSO model with a larger value for the minimum luminosity at $z = 0$ and a slightly steeper tail-end slope than the standard model, can simultaneously provide a fair match to the observed helium opacity and hydrogen photoionisation rate measurements when one includes a realistic soft contribution from galaxies. It is important to point out, however, that the specific examples chosen in this paper represent a degenerate class of models which can also be combined to produce similar results. More specifically, in the case of quasars, the parameters $L_{\rm min,0}$ and α_{QSO} can both be adjusted to deliver the required ionising emissivity in helium while changing the resultant ionising emissivity in hydrogen. This would therefore create a large set of different galactic models which would also be fairly successful at reproducing the observations. In Figure 7, we demonstrate this degeneracy by plotting the absolute value of the difference between the logarithms of the computed hydrogen photoionisation rate ($\Gamma_{\rm HI}$) and the measured value obtained by Rauch et al. (1997) ($\Gamma_{{\rm HI},m}$) as a function of quasar parameters $L_{\rm min,0}$ and $\alpha_{\rm QSO}$ at redshifts 3 and 4. The labeled contours in each panel show the percent difference from the corresponding measured value. To tie in the correlation with the helium observations, we also plot in each panel the curve (*white-dashed line*) in the $L_{\rm min,0}$-$\alpha_{\rm QSO}$ plane that produces the same number of He II ionising photons as quasar Model 5 from SAH. The success of the latter model in matching He II opacity measurements and the strong correlation between the number of ionising photons released and the resulting opacities, effectively restricts us to consider models only in the vicinity of this curve. The plots make it apparent that a pure quasar model based on the adopted LF, while capable of producing agreement at $z = 3$, fails by a large factor at $z = 4$ for any reasonable range in $L_{\rm min,0}$ and $\alpha_{\rm QSO}$. On the other hand, as the bottom panels indicate, a quasar model which is supplemented with an additional soft component, which in this case is galactic Model M2, is able to significantly reconcile this failure. It is important to point out to the reader that Figure 7 is based on relatively sparse data in both H I and He II (7 and 4 quasar spectra, respectively) and that more observations, especially at high redshift, are necessary to place definitive constraints on the models.

7. CONCLUSION

In this paper, we have utilised observations in both H I and He II to estimate the contributions to the UV background from quasars and galaxies. The fact that only quasars are capable of producing radiation hard enough to ionise He II has allowed us to select a particular quasar model based solely on the He II opacity measurements, independent of the galactic model. Including measurements of the photoionisation rate in H I between $2.5 \lesssim z \lesssim 4.5$ then enables us to study predictions based on two hotly debated models for the galactic contribution.

We find that a quasar model with less emission than the widely quoted "standard" model in conjunction with a galactic model with a slightly rising SFR that contributes a comparable amount of H I ionising radiation at $z \simeq 3$, is necessary to achieve good agreement with all relevant observations. Such a composite model makes it much easier to understand how the intergalactic medium can remain highly ionised at redshifts $z > 4$ where the contribution from bright quasars falls off significantly. It can also explain the apparent progressive softening of the UV background at $z > 3$ as suggested by metal absorption line observations (Savaglio et al. 1997; Songaila 1998). The particular choice for the galactic component in the above model is further bolstered by the fact that the galactic model appears to match observations for the emissivity of LBGs between $2.5 \lesssim z \lesssim 4.5$ as it appears as if the adopted galactic model M2 offers good agreement with the observations if the typical value for $f[1500]/f[900]$ lies somewhere between the values measured by Steidel et al. (2001) and Giallongo et al. (2002). Moreover, the rise in the SFR beyond $z \sim 3$ is in accord with some observations and theoretical predictions (for a discussion, see e.g. Springel & Hernquist 2002a).

We have also shown that there exists a degenerate class of quasar models which are equally successful at matching the He II observations while producing a large dispersion in their H I contributions. However, the particular QSO model adopted in this paper has the interesting property of being characterised by plausible values for $L_{\rm min}$ and α_s while naturally requiring an extra galactic component that seems to be consistent with observations of both its amplitude and shape.

While the scenario presented in this paper appears promising, we must emphasise that it is based on relatively sparse data. Future observations gathered with the Sloan Digital Sky Survey (SDSS) will allow us to reduce the uncertainties associated with quasar models at high redshifts. Coupled with future measurements of the proximity effect and the evolution of the intensity ratio of metal lines, it should soon be possible to place even tighter constraints on the relative contributions from quasars and galaxies to the UV background at $z \sim 2.5 - 5$.

We thank Kentaro Nagamine for providing us with data related to the SFRs of LBGs in a convenient and useful form as well as providing useful comments regarding the nature of galactic sources. We also thank Volker Springel for comments on the manuscript, Martin Elvis for informative discussions concerning the specifics of quasar SEDs in the context of our analysis, Kurt Adelberger for useful discussions about the UV emissivity of LBGs, and George Rybicki for discussions related to radiative processes. A.S. thanks Daniel Harvey for many constructive discussions related to this study. This work was supported in part by NSF grants ACI96-19019, AST-9803137, and PHY 9507695.

REFERENCES

Abel, T., Haehnelt, M. G. 1999, ApJ, 520, L13

Anderson, S. F., Hogan, C. J., Williams, B. F., & Carswell, R. F. 1999, AJ, 117, 56

Becker, R. H., Fan, X., White, R. L., Strauss, M. A., Narayanan, V. K., Lupton, R. H., Gunn, J. E., Annis, J., Bahcall, N. A., Connolly, A. J., Csabai, I., Czarapata, P. C., Doi, M., Heckman, T. M, Hennessy, G. S., Knapp, G. R., Lamb, D.Q., Nash, T., Nichol, R., McKay, T. A., Munn, J. A., Pier, J. R., Richards, G. T., Schneider, D. P., Stoughton, C., Szalay, A. S., Thakar, A. R. 2001, AJ, 122, 2850

Bernardi, M., Sheth, R.K., Subbarao, M., Richards, G.T., Burles, S., Connolly, A.J., Frieman, J., Nichol, R., Schaye, J., Schneider, D.P., Vanden Berk, D.E., York, D.G., Brinkmann, J. & Lamb, D.Q. 2002, AJ, submitted, [astro-ph/0206293]

Bianchi, S., Cristiani, S., Kim, T.S. 2001, A&A, 376, 1B

Boyle, B. J., Shanks, T., Georgantopoulos, I., et al. 1994, MNRAS, 271, 639

Boyle, B. J., Shanks, T., & Peterson, B. A. 1988, MNRAS, 235, 935

Brinkmann, W., Yuan, W., & Siebert, J. 1997, A&A, 319, 413

Cen, R., Miralda-Escudé, J., Ostriker, J.P. & Rauch, M. 1994, ApJ, 427, L9

Cheng F.-Z., Danese L., De Zotti G., Franceschini, A. 1985, MNRAS, 212, 857

Connolly, A. J., Szalay, A. S., Dickinson, M. E., Subbarao, M. U., & Brunner, R. J. 1997, ApJ, 486, L11

Cooke, A. J., Espey, B., & Carswell, R.F. 1997, MNRAS, 284, 552

Cowie, L. L., Songaila, A., & Barger, A. J. 1999, AJ, 118, 603

Croft, R.A.C., Weinberg, D.H., Katz, N. & Hernquist, L. 1997, ApJ, 488, 532

Croft, R.A.C., Di Matteo, T., Davé, R., Hernquist, L., Katz, N., Fardal, M.A. & Weinberg, D.H. 2001, ApJ, 557, 67

Davé, R., Hernquist, L., Katz, N. & Weinberg, D.H. 1999, ApJ, 511, 521

Davé, R., Cen, R., Ostriker, J.P., Bryan, G.L., Hernquist, L., Katz, N., Weinberg, D.H., Norman, M.L., & O'Shea, B. 2001, ApJ, 552, 473

Davidsen, A. F., Kriss, G. A., & Zheng, W. 1996, Nature, 380, 47

Devriendt, J. E. G., Sethi, S. K., Guiderdoni, B., & Nath, B. B. 1998, MNRAS, 298, 708

Francis, P. J., Hewett, P. C., Foltz, C. B., Chaffee, F. H., Weymann, R. J., & Morris, S. L. 1991, ApJ, 373, 465

Giallongo, E., Cristiani, S., D'Odorico, S., Fontana, A. 2002, preprint [astro-ph/0202293]

Giallongo, E., Cristiani, S., D'Odorico, S., Fontana, A., & Savaglio, S. 1996, ApJ, 466, 46

Giallongo, E., Fontana, A., & Madau, P. 1997, MNRAS, 289, 629

Haardt, F. & Madau, P. 1996, ApJ, 461, 20

Haiman, Z., & Menou, K. 2000, ApJ, 531, 42

Heap, S. R., Williger, G. M., Smette, A., Hubeny, I., Sahu, M. S., Jenkins, E. B., Tripp, T. M., Winkler, J. N. 2000, ApJ, 534, 69

Hernquist, L., Katz, N., Weinberg, D.H., & Miralda-Escudé, J. 1996, ApJ, 457, L51

Hui, L., Gnedin, N. Y., 1997, MNRAS 292, 27

Jakobsen, P., Boksenberg, A., Deharveng, J. M, Greenfield, P., Jedrzejewski, R., & Paresce, F. 1994, Nature, 370, 35

Katz, N., Weinberg, D.H., & Hernquist, L. 1996, ApJS, 105, 19

Kauffmann, G., & Haehnelt, M. 2000, MNRAS, 311, 576

Kim, T. S., Cristiani, S., & D'Odorico, S. 2001, A&A, 373, 757

Kim, T.-S., Hu, E. M., Cowie, L. L., & Songaila, A. 1997, AJ, 114, 1

Kriss, G. A., Shull, J. M., Oegerle, W., Zheng, W., Davidsen, A. F., Songaila, A., Tumlinson, J., Cowie, L. L., Deharveng, J.-M., Friedman, S. D., Giroux, M. L., Green, R. F., Hutchings, J. B., Jenkins, E. B., Kruk, J. W., Moos, H. W., Morton, D. C., Sembach, K. R., Tripp, T. M. 2001, Science, 293, 5532

Lilly, S. J., LeFévre, O., Hammer, F., &Crampton, D. 1996, ApJ, 460, L1

Machacek, M. E., Bryan, G. L., Meiksin, A., Anninos, P., Thayer, D., Norman, M., & Zhang, Y. 2000, ApJ, 532, 118

Madau, P.. 1997, in AIP Conf. Proc. 393, Star Formation Near and Far, ed. S. S. Holt & G. L. Mundy (New York: AIP), 481

Madau, P., Ferguson, H. C., Dickinson, E. D., Giavalisco, M., Steidel, C. C., & Fruchter, A. 1996, MNRAS, 283, 1388

Madau, P., Haardt, F., Rees, M. J. 1999, ApJ, 514, 648

Madau, P., Pozzetti, L., & Dickinson, M. 1998, ApJ, 498, 106

Nagamine, K., Cen, R., Ostriker, J. P. 2000, ApJ, 541, 25

Osterbrock, D. E. 1989, Astrophysics of Gaseous Nebular and Active Galactic Nuclei (Mill Valley: University Science)

Paresce, F., McKee, C., & Bowyer, S. 1980, ApJ, 240

Pascarelle, S. M., Lanzetta, K. M., & Fernandez-Soto, A. 1998, ApJ, 508, L1

Peebles, P. J. E. 1993, Principals of Physical Cosmology (Princeton: Princeton Univ. Press)

Pei, Y. C. 1995, ApJ, 438, 623

Rauch, M., Miralda-Escudé, J., Sargent, W. L. W., Barlow, T. A., Weinberg, D. H., Hernquist, L., Katz, N., Cen, R., Ostriker, J. P. 1997, ApJ, 489, 7

Reimers, D., Köhler, S., Wisotzki, L., Groote, D., Rodriguez-Pascal, P., Wamsteker, W. 1997, A&A, 327, 890

Ricotti, M., Gnedin, N. Y., & Shull, J. M. 2000, ApJ, 534, 41

Sargent, W. L. W., Steidel, C. C., & Boksenberg, A. 1989, ApJS, 69, 703

Savaglio, S., Cristiani, S., D'Odorico, S., Fontana, A., Giallongo, E., Molaro, P., 1997, A&A, 318, 347

Sawicki, M. J., Lin, H., & Yee, H. K. C. 1997, AJ, 113, 1

Scott, J., Bechtold, J., Dobrzycki, A., & Kulkarni, V. P. 2000, ApJS, 130, 67

Shull, J. M., Roberts, D., Giroux, M. L., Penton, S. V., & Fardal, M. A. 1999, AJ, 115, 2184

Smette, A., Heap, S. R., Williger, G. M., Tripp, T. M., Jenkins, E. B., Songaila, A. 2002, ApJ, 564, 542

Sokasian, A., Abel, T. & Hernquist, L. 2001, NewA, 6, 359

Sokasian, A., Abel, T. & Hernquist, L. 2002, MNRAS, 332, 601 [SAH]

Songaila, A. 1998, ApJ, 115, 2184

Springel, V., Yoshida, N., White, S. D. M. 2001, NewA, 6, 795

Springel, V., White, M. & Hernquist, L. 2001, ApJ, 549, 681

Springel, V. & Hernquist, L. 2002a, MNRAS, submitted [astro-ph/0206395]

Springel, V. & Hernquist, L. 2002b, MNRAS, 333, 649

Springel, V. & Hernquist, L. 2002c, MNRAS, submitted [astro-ph/0206393]

Steidel, C. C., Adelberger, K. L., Giavalisco, M., Dickinson, M., & Pettini, M. 1999 , ApJ, 519, 1

Steidel, C. C., Pettini, M., & Adelberger, K. L. 2001, ApJ, 546, 665

Stengler-Larrea, E. A., Boksenberg, A., Steidel, C. C., Sargent, W. L. W., Bahcall, J. N., Bergeron, J., Hartig, G. F., Jannuzi, B. T., Kirhakos, S., Savage, B. D., Schneider, D. P., Turnshek, D. A., Weymann, R. J. 1995, ApJ, 444, 64

Telfer, R. C., Zheng, W., Kriss, G. A., Davidsen, A. F. 2002, ApJ, 565, 773

Theuns, T., Zaroubi, S., Kim, T., Tzanavaris, P., & Carswell, R. F. 2002a, MNRAS, 332, 367

Theuns, T., Bernardi, M., Frieman, J., Hewett, P., Schaye, J., Sheth, R.K. & Subbarao, M. 2002b, ApJ, submitted [astro-ph/0206319]

Treyer, M. A., Ellis, R. S., Millard, B., Donas, J., & Bridges, T. J. 1998, MNRAS, 300, 303

Weymann, R. J., Jannuzi, B. T., Lu, L., Bahcall, J. N., Bergeron, J., Boksenberg, A., Hartig, G. F., Kirhakos, S., Sargent, W. L. W., Savage, B. D., Schneider, D. P., Turnshek, D. A., & Wolfe, A. M. 1998, ApJ, 506 1

Yuan, W., Siebert, J., & Brinkmann, W. 1998, A&A, 334, 498

Zhang, Y., Anninos, P. & Norman, M.L. 1995, ApJ, 453, L57

Zheng, W., Kriss, G. A., Telfer, R. C., Crimes, J. P., & Davidsen, A.F. 1998, ApJ, 492, 855

TABLE 1

Quasar Source Parameters

Quasar Model	$T_{\rm life}$ [10^7 yrs]	$L_{\rm min,0}$ [$10^9 L_{B,\odot}$]	$M_{\rm min}$ [$10^{10} M_\odot$]	β [radians]	$\alpha_{\rm QSO}$
1	2.0	3.91	1.8	π	1.8
5	2.0	23.5	1.8	π	1.9

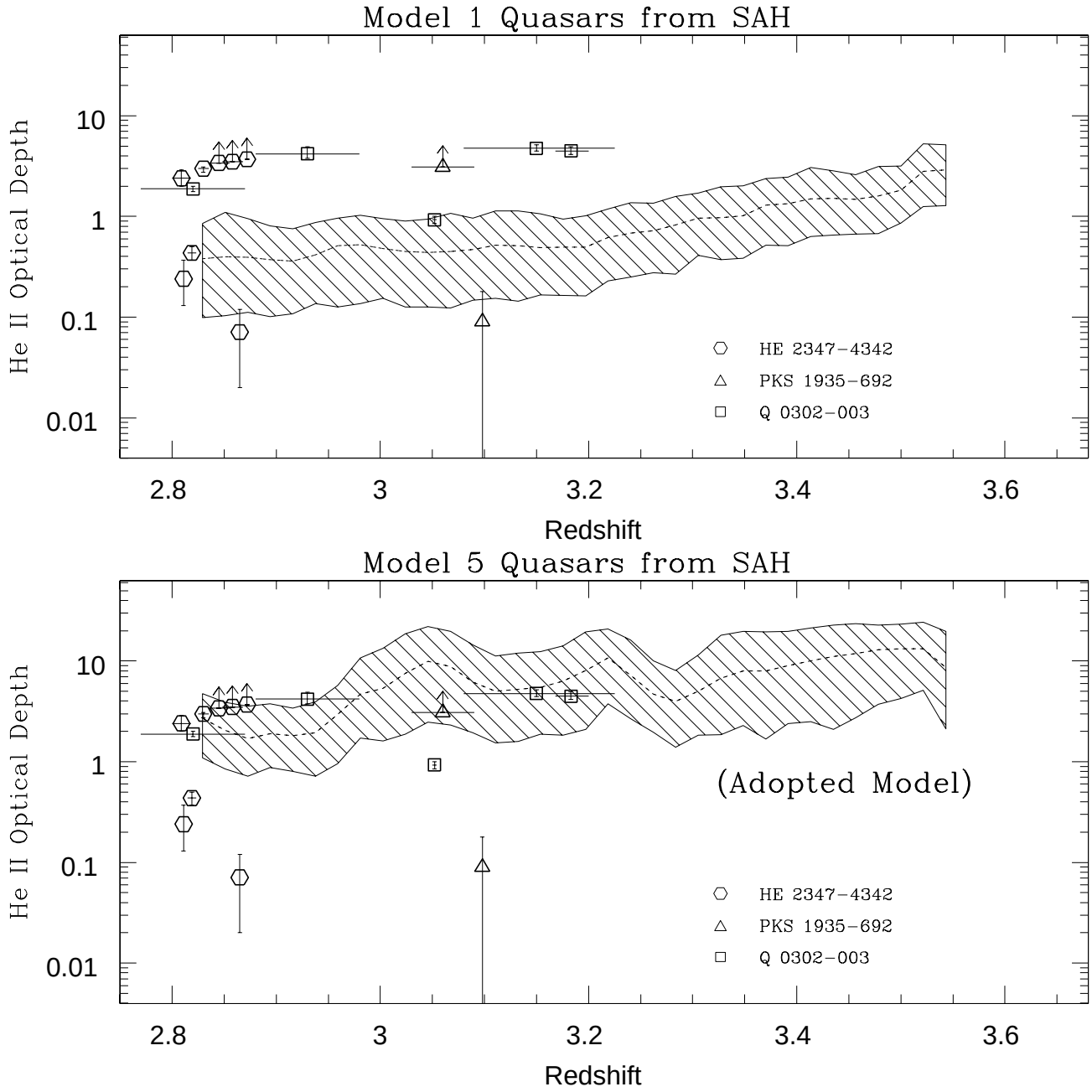

Fig. 1.— Redshift evolution of the effective mean optical depth of He II absorption in Models 1 and 5 from SAH. Hatched regions represent the optical depth derived from the simulations at the 90% confidence level with the dashed lines indicating mean values. Observational results from quasars HE 2347-4342, PKS 1935-692 and Q 0302-003 are plotted for comparison. We adopt Model 5 for our analysis in this paper.

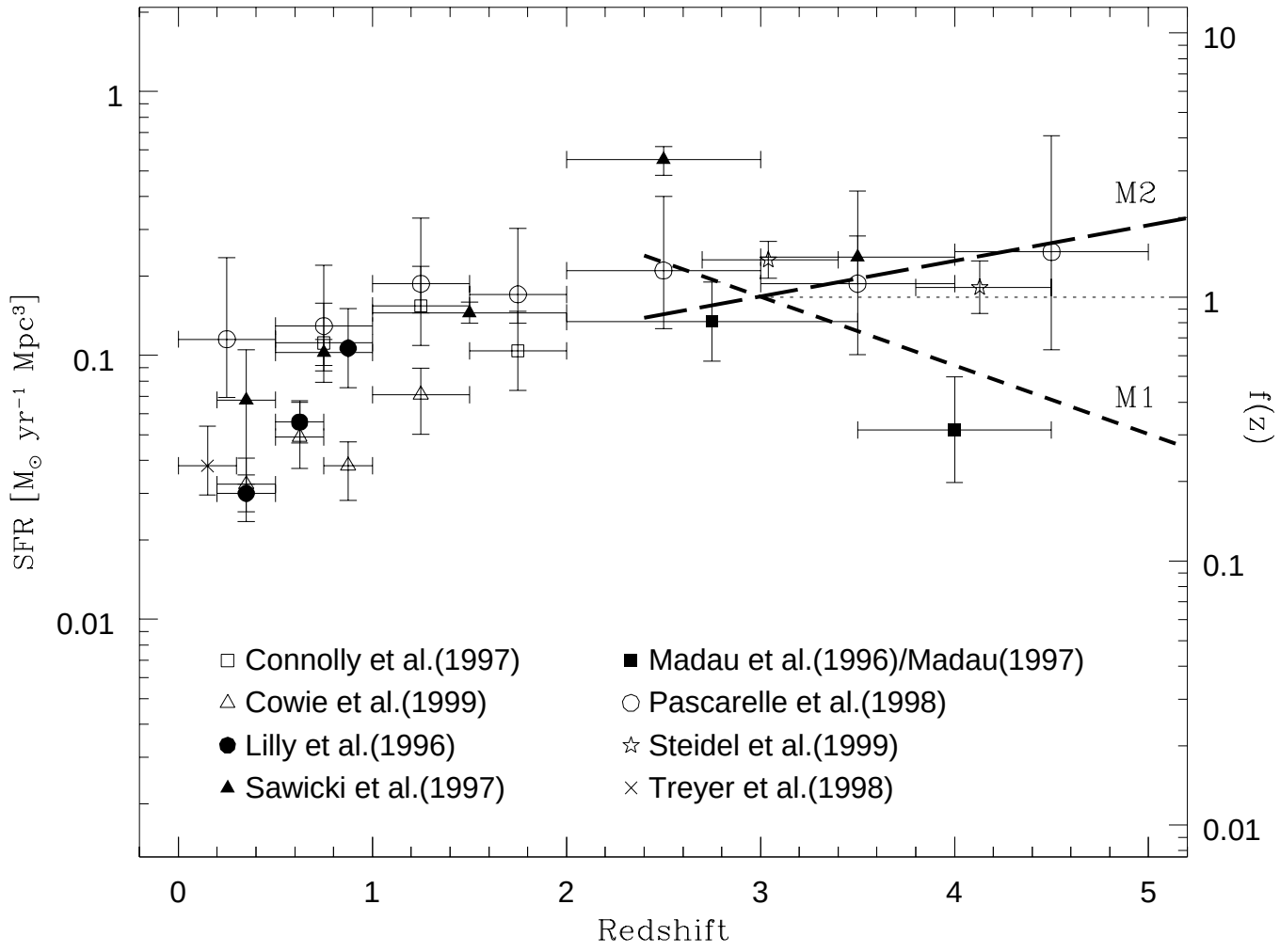

Fig. 2.— Extinction-corrected data points for the comoving SFR in a flat Λ cosmology with parameters (Ω_m, Ω_Λ)=(0.37, 0.63) and $h = 0.7$ as summarised by Nagamine, Cen, & Ostriker (2000). Sources for the raw data are listed above according to their corresponding points. The bold short-dashed and long-dashed lines represent Models 1 (M1) and 2 (M2) for our comoving redshift evolution factor $f(z)$ (right axis), respectively. Note that $f(z)$ is normalised to unity at $z = 3$ for both models, in accord with our parameterisation of the comoving galactic emissivity: $\epsilon_{\rm GAL,c}(\nu, z) = \epsilon_{\rm GAL,c}(\nu_{\rm HI}, 3)\ f(z)\ (\nu/\nu_{\rm HI})^{-\alpha_{GAL}}$.

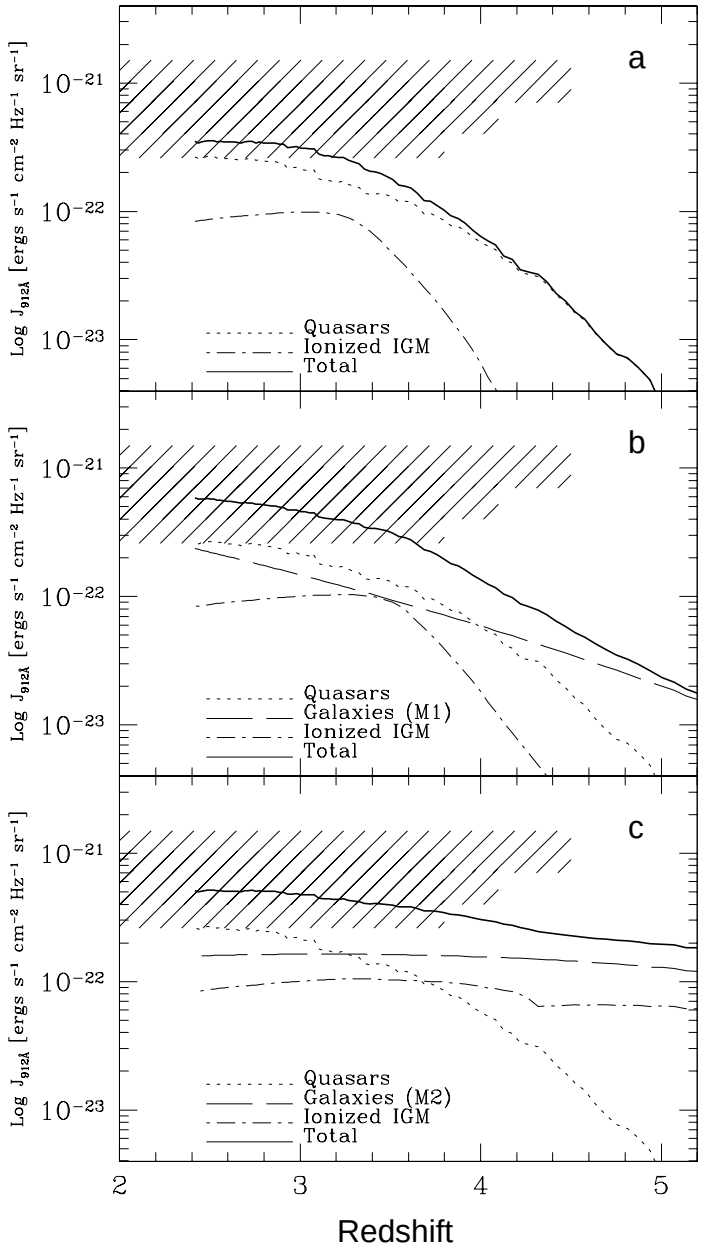

Fig. 3.— Background intensity at $\lambda = 912$ Å resulting from (a) quasars only, (b) quasars and galactic Model M1, and (c) quasars and galactic Model M2. Shown are the separate contributions from quasars (dotted), galaxies (dashed), and the ionised IGM (dashed-dotted). The shaded region refers to the Lyman limit background estimated from the proximity effect (Giallongo et al. 1996; Cooke et al. 1997; Scott et al. 2000)

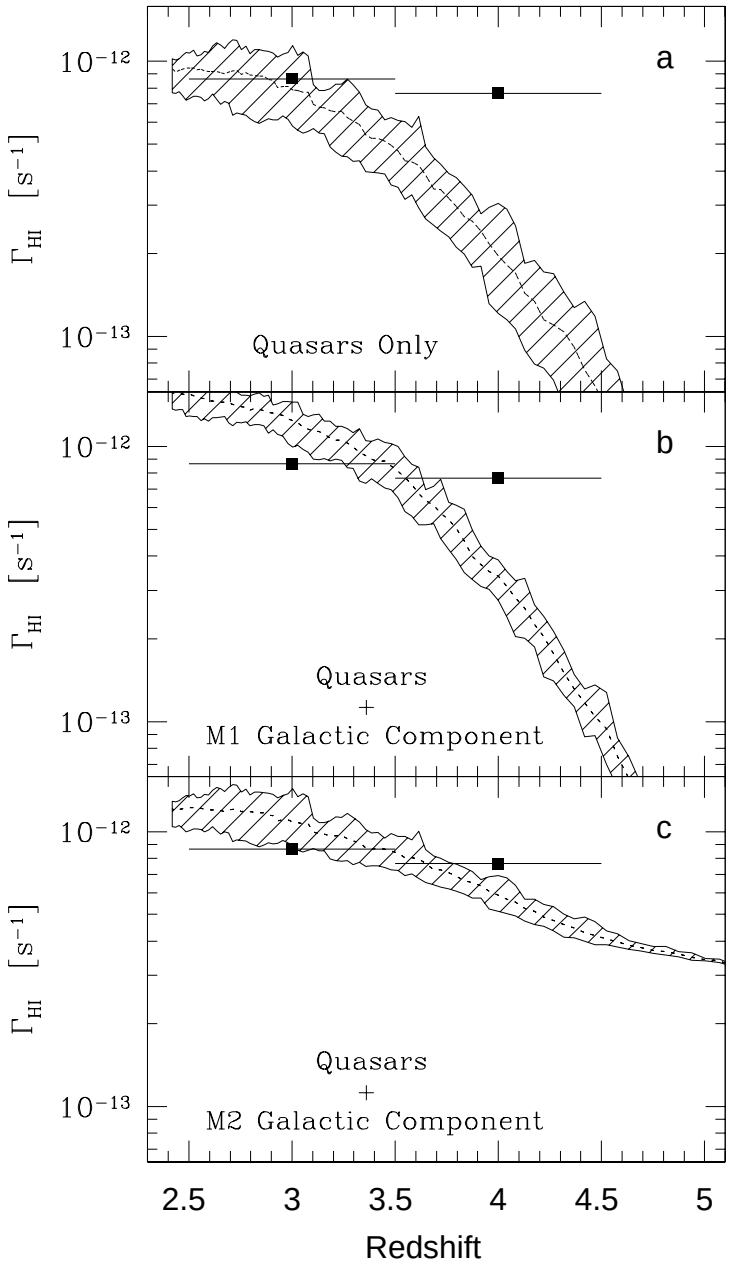

Fig. 4.— Hydrogen photoionisation rate as a function of redshift resulting from (a) quasars only, (b) quasars and galactic Model M1, and (c) quasars and galactic Model M2. Hatched regions represent the range of values corresponding to the 90% confidence level from repeating the analysis with 30 unique random seeds associated with the quasar selection algorithm. The two data points represent measurements of Γ_{HI} over the indicated redshift ranges (horizontal lines) obtained by Rauch et al. (1997), after being adjusted for the cosmology used in this paper (see text).

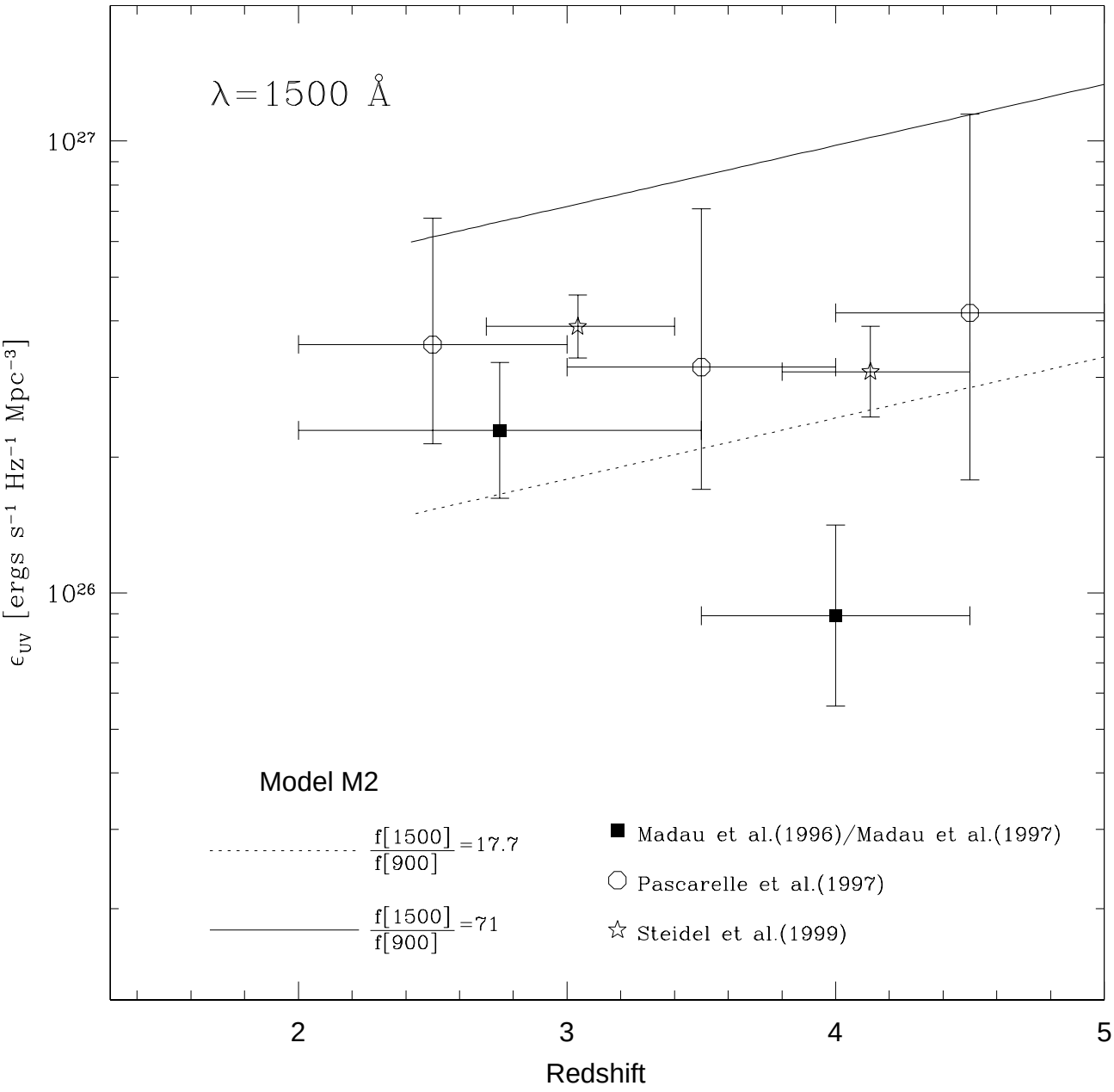

Fig. 5.— Comoving emissivity at $\lambda = 1500$ Å from our galactic Model M2 as a function of redshift based on the two values of the observed flux ratio from Steidel et al. (2001) (dotted line) and Giallongo et al. (2002) (solid line). Also plotted are the relevant observations of the UV emissivity at $\lambda = 1500$ Å from Steidel et al. (1999), Pascarelle et al. (1998), Madau et al. (1996), and Madau et al. (1998) adjusted for a flat Λ cosmology: (Ω_m, Ω_Λ)=(0.37, 0.63) and $h = 0.7$ (corrected data obtained from Nagamine, Cen, & Ostriker [2000]).

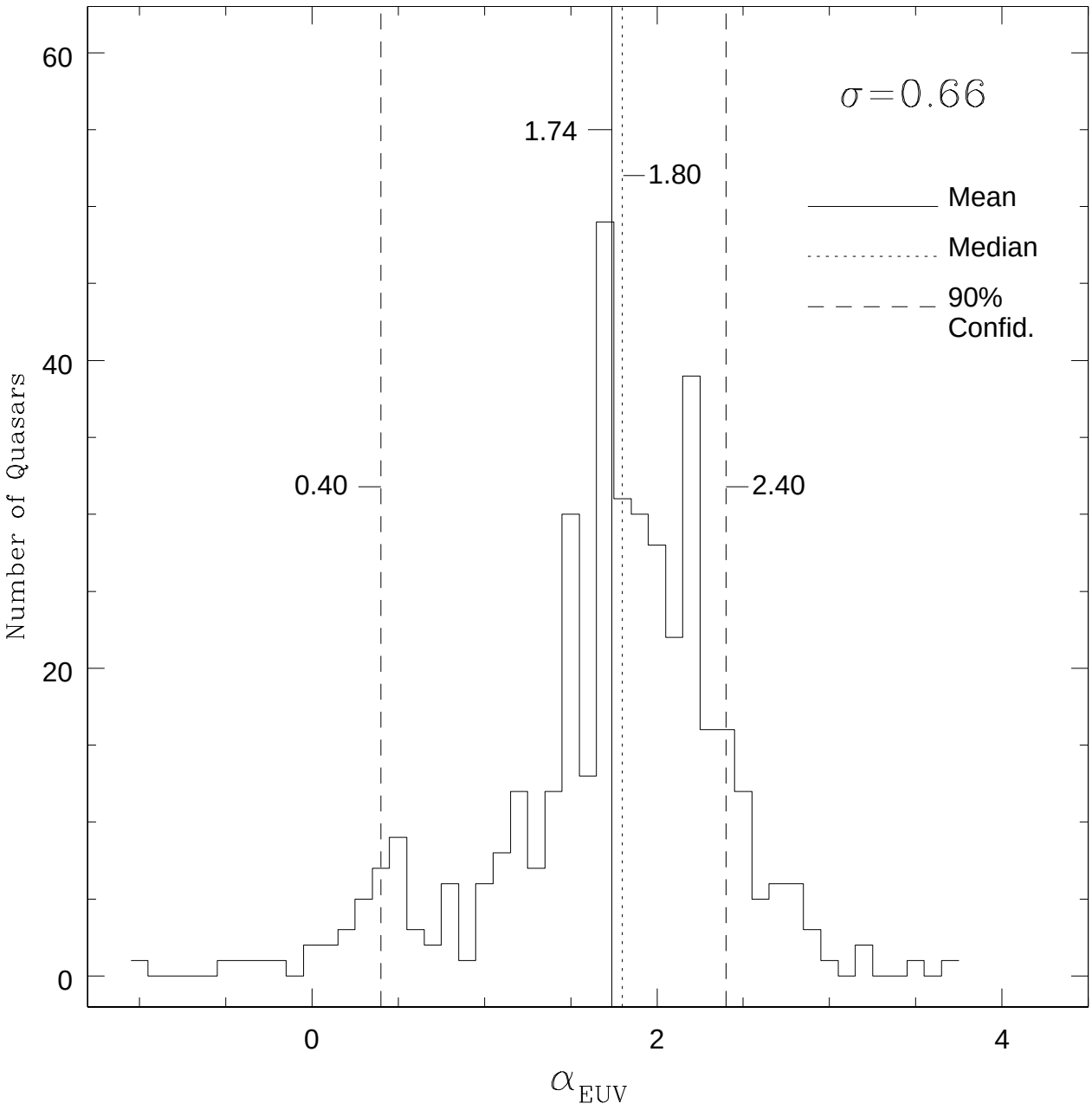

Fig. 6.— Quasar EUV spectral index distribution compiled from the data in Telfer et al. (2002). The distribution includes results for subsamples of radio-quiet and radio-loud QSOs (see text). The indices are defined as $f(\nu) \propto \nu^{-\alpha}$ between 500 and 1200 Å. The mean, median, and rms deviation (σ) of the distribution are indicated.

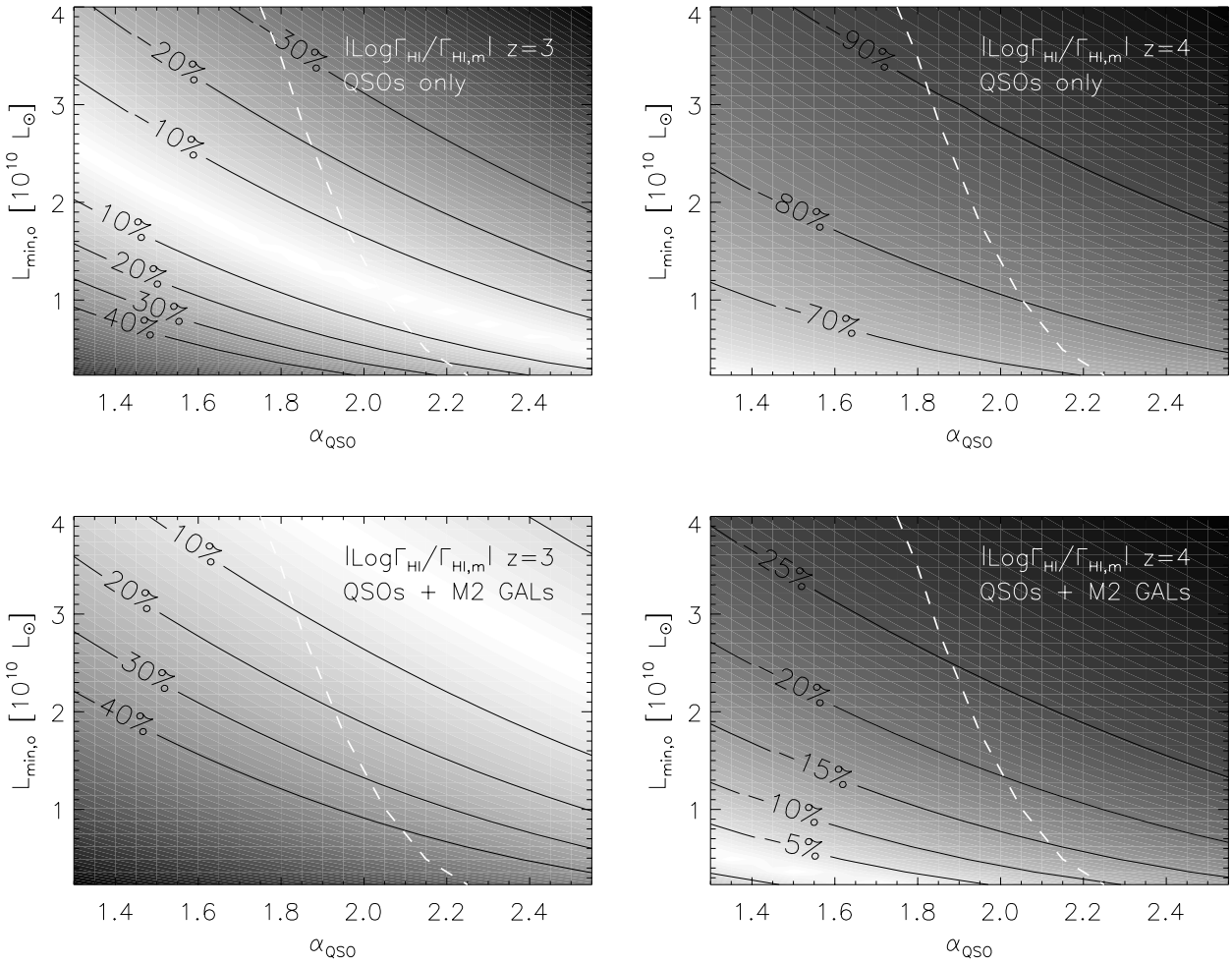

Fig. 7.— Greyscale plots showing the absolute value of the difference between the logarithms of the computed hydrogen photoionisation rate, $\Gamma_{\rm HI}$, and the measured value obtained from Rauch et al. (1997), $\Gamma_{{\rm HI},m}$, as a function of quasar parameters $L_{\rm min,0}$ and $\alpha_{\rm QSO}$ at redshifts 3 and 4. The top panels show the results for the case with only quasars while the bottom panels show the results for quasars with M2 galaxies included. The labeled contours in each panel show the percent difference from the corresponding measured value. Also plotted in each panel is the curve (*white-dashed line*) in the $L_{\rm min,0}$-$\alpha_{\rm QSO}$ plane that would produce the same number of He II ionising photons as quasar Model 5 from SAH.

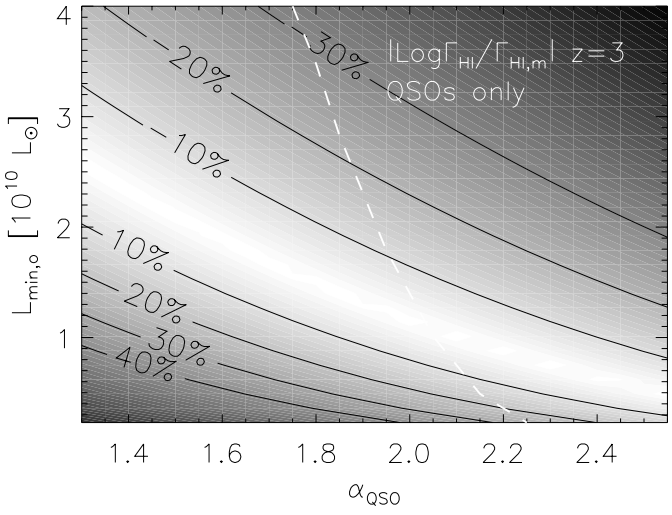
|LogΓ_HI/Γ_HI,m| z=3
QSOs only
30%
20%
10%
10%
20%
30%
40%
L_min,o [10^10 L_⊙]
α_QSO

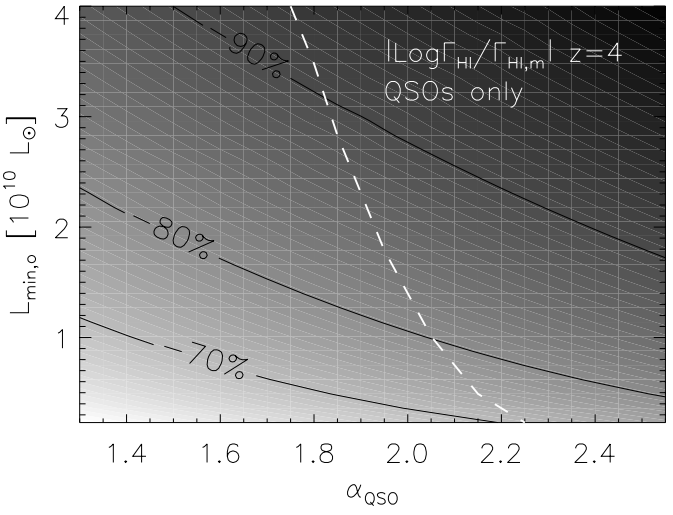
|LogΓ_HI/Γ_HI,m| z=4
QSOs only
90%
80%
70%
L_min,o [10^10 L_⊙]
α_QSO

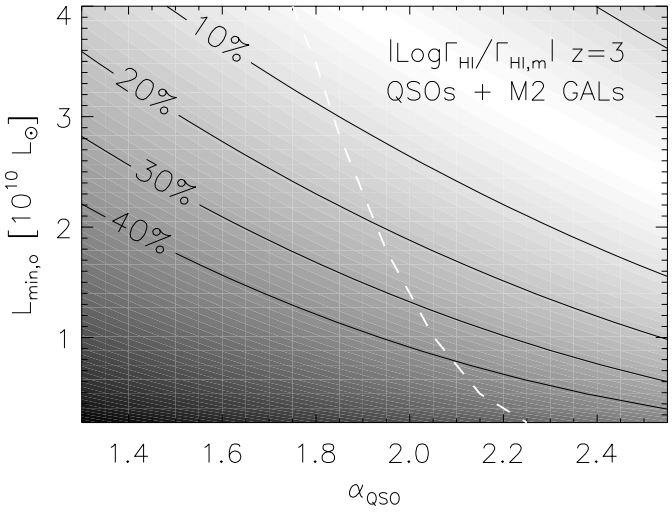
|LogΓ_HI/Γ_HI,m| z=3
QSOs + M2 GALs
10%
20%
30%
40%
L_min,o [10^10 L_⊙]
α_QSO

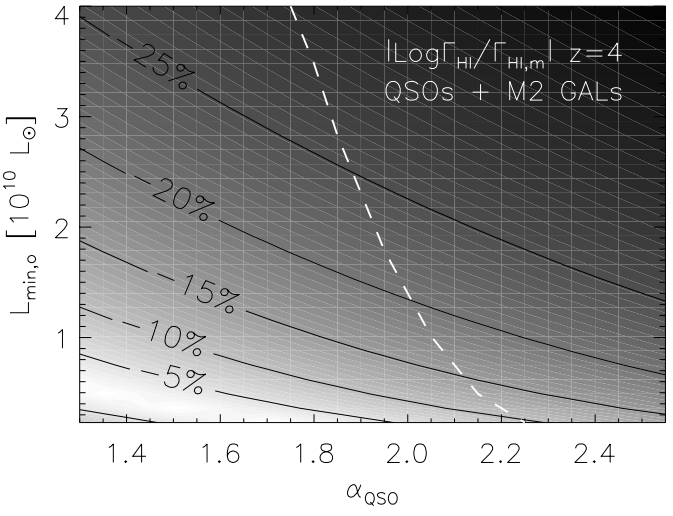
|LogΓ_HI/Γ_HI,m| z=4
QSOs + M2 GALs
25%
20%
15%
10%
5%
L_min,o [10^10 L_⊙]
α_QSO